Nanostructured Zinc Oxide Gas Sensors

Spencer Cooper, Nicholas Barmore, Foster Boom, and Steven N. Girard

Department of Chemistry, University of Wisconsin-Whitewater

Abstract

Metal oxide semiconductors are used as gas sensors in a variety of spaceflight applications to detect the presence of various gases. Here, we report the synthesis, characterization, and sensor development of nanostructured zinc oxide (ZnO) semiconductors for gas sensing of CO_2 and O_2. Using a general hydrothermal reaction between zinc precursor salts (zinc nitrate, sulfate, acetate, and chloride) and a base (hexamethylenetetramine) at concentrations between 0.05 and 1.0 M, we show that nanostructured zinc oxide crystals can be grown directly onto glass substrates. The nanostructures generated vary significantly in size, morphology, and surface area depending on reagent and concentrations used, including nanorods (zinc acetate), nano-honeycombs (zinc nitrate), and nanoplates (zinc sulfate). We also report improvements to the adhesion and film homogeneity via spray pyrolysis, wherein substrates are pre-treated with an aerosolized spray of zinc salt precursors at high temperature. Lastly, we present the development of ZnO-coated substrates as CO_2 sensors via preliminary resistance measurements in air and under CO_2.

Introduction

Gas sensors are vital on spacecraft for the sensing of a variety of gases, including O_2, H_2, CO, CO_2, and volatile organics (VOCs). During space flight, exposure to harmful gas could prove fatal to both the crew and spacecraft. A variety of sensor technologies can be used to detect gases, including metal oxide semiconductors. Metal oxide semiconductors (MOS) gas sensors are of particular interest due to their ease in synthesis, low cost and toxicity, and high sensitivity and selectivity to gases. Examples of MOS being utilized right now are SnO_2, TiO_2, and ZrO_2 (NASA, Glenn Research Center). In practice, MOS sensors can detect the adsorption of gases by changes in the electrical transport of the metal oxide. For example, zinc oxide (ZnO) is an interesting MOS sensor that can be used to sense CO_2 and O_2. Its synthesis is simple, using non-toxic and naturally abundant materials. Furthermore, ZnO can be easily synthesized as nanostructures, around 1-100 nm, which enhances the sensing capabilities through significant enhancements in surface area.

Prior studies show ZnO responds to CO_2 adsorption via a decrease in the electrical resistance of the ZnO film. ZnO is a wide band gap (E.g. = 3.3 eV) intrinsically n-type semiconductor caused by oxygen vacancies at the surface level (Korotcenkov et al.). It has been hypothesized that in air, adsorbed O_2 onto the ZnO surface can become reduced from electrons in the conduction band through photoexcitation. This process forms adsorbed O^{2-} ions, and the reduction of carriers in the conduction band increases the ZnO resistance. Conversely, when ZnO is exposed to CO_2, the absence of O_2 decreases resistance. Additionally, it is theorized that metastable carbon intermediates (such as carbon trioxide, CO_3) can form. When the carbon intermediates decompose, reducing electrons can be injected into the conduction band of the ZnO film, further decreasing its resistance (Kanaparthi et al.).

Here, we report the development of a simple chemical process to grow ZnO nanostructures onto glass substrates. ZnO may be precipitated using a simple synthetic approach wherein a zinc salt containing soluble Zn^{2+} ions is reacted with an aqueous basic solution. The reaction to generate ZnO proceeds:

Funding provided by the Wisconsin Space Grant Consortium (HEI21_3-0) made available through NASA Education Cooperative Agreement #80NSSC20M0123 and the UWW Undergraduate Research Program.

$$Zn^{2+}(aq) + 2OH^{-}(aq) \rightarrow Zn(OH)_2(s) + heat \rightarrow ZnO(s) + H_2O(g)$$

The zinc salts used must be water soluble, such as zinc sulfate, nitrate, acetate, and chloride. The basic reagent chosen is hexamethylenetetramine, $(CH_2)_6N_4$ (HMT, Figure 1), which decomposes slowly into ammonium hydroxide via a two-step reaction pathway:

$$(CH_2)_6N_4(aq) + 6H_2O(l) \rightarrow 6\ H_2CO\ (aq) + 4\ NH_3(aq)$$
$$NH_3\ (aq) + H_2O(l) \rightarrow NH_4^{+}\ (aq) + OH^{-}\ (aq)$$

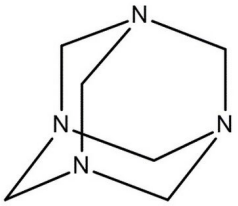

Figure 1. Molecular structure of hexamethylenetetramine (HMT) molecule.

The slow decomposition of HMT results in kinetic control of the precipitation reaction, slowly producing ZnO and promoting growth at the nanoscale. Depending on differences in reagent concentration, temperature, and supersaturation, different nanostructured morphologies can be observed.

Growing ZnO directly into the substrate increases adherence and interaction with the substrate while undergoing resistance testing. This way, the natural crystal growth and differences in morphology can be analyzed and compared between each precursor salt to determine which has the most surface area of active sites for CO_2 interaction. However, this also means that the synthesis process is more complex when it comes to procuring a high-quality coating.

Materials and Methods

Synthesis. Zinc salts and HMT were combined in equimolar concentrations varying from 0.1 M to 1.0 M, each at 10 mL, and mixed together, in a 50 mL Falcon centrifuge tube. A borosilicate glass slide was added to the centrifuge tube, and the tube was capped. The tubes were placed in an oven and heated to 90 °C for 24 hours. Following the reaction, selected samples were annealed at 350 °C for 24 hours to fully transform the film into crystalline ZnO. The as-deposited nanostructured ZnO films had the appearance of white powder deposited onto the glass slide, Figure 2A. Upon completion of the hydrothermal reaction, all samples were cleaned with deionized water and rinsed with ethanol and dried under air.

Spray Pyrolysis. To improve ZnO film adhesion to the substrates, we performed spray pyrolysis. For this process, a substrate was heated on a hot plate to ~200 °C. The substrate was then sprayed using a conventional aerosol mister approximately 30 times from ~25 cm distance with a 1.0 M aqueous zinc salt solution (same composition as above), Figure 2B. A couple seconds was given in between each spray to allow the liquid solution to fully evaporate before adding more liquid to prevent the glass from cracking.

Figure 2. A ZnO sample displaying excellent coverage on glass substrate (A). Spray pyrolysis setup (B)

Powder X-Ray Diffraction. Powder X-Ray Diffraction analysis was accomplished using a Rigaku MiniFlex Desktop X-Ray Diffractometer, using Cu-K_α radiation ($\lambda = 1.5418$ Å). Samples were analyzed in the 2θ range of 30 to 60 degrees. Diffractograms were used to determine 2θ and β (full-width-at-half-maximum) peak value. This data was used to analyze the average particle diameter, d-spacing, and *a* and *c* lattice parameters of each sample.

Scanning Electron Microscopy. A JEOL JSM-6390 scanning electron microscope operating at 30 kV in secondary electron mode was utilized to get high quality images of the nanostructured crystals and determine crystal morphology.

Resistance measurements. Electrical transport measurements of ZnO nanostructured film resistance were obtained via a 2-wire and 4-wire measurement systems using carbon coated conductive sponges spaced approximately 3 mm apart, Figure 3. The resistance was measured using a Keithley Sourcemeter with a maximum range of 1 GΩ. Later experiments utilized a spring-loaded 4 probe resistance measurement system.

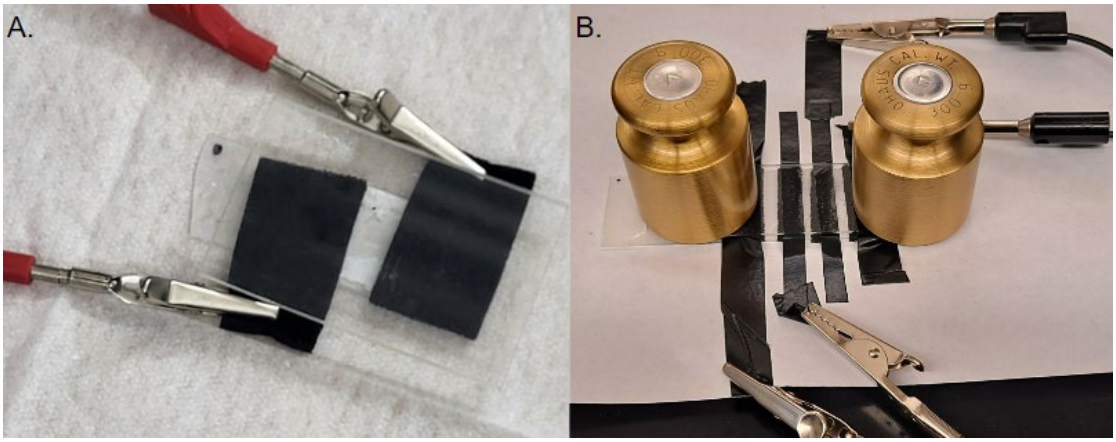

Figure 3. 2-wire (A) and 4-wire (B) carbon sponge measurement system.

CO_2 testing. To measure response to CO_2 gas, a gas tank (>99% CO_2) fitted with a regulator and plastic tubing was purged over the obtained ZnO nanostructured film substrates at an outlet pressure of ~1 psi. Samples were measured under a 2 and 4-point spring loaded gold pin measurement jig with probes connected to a sourcemeter, Figure 4.

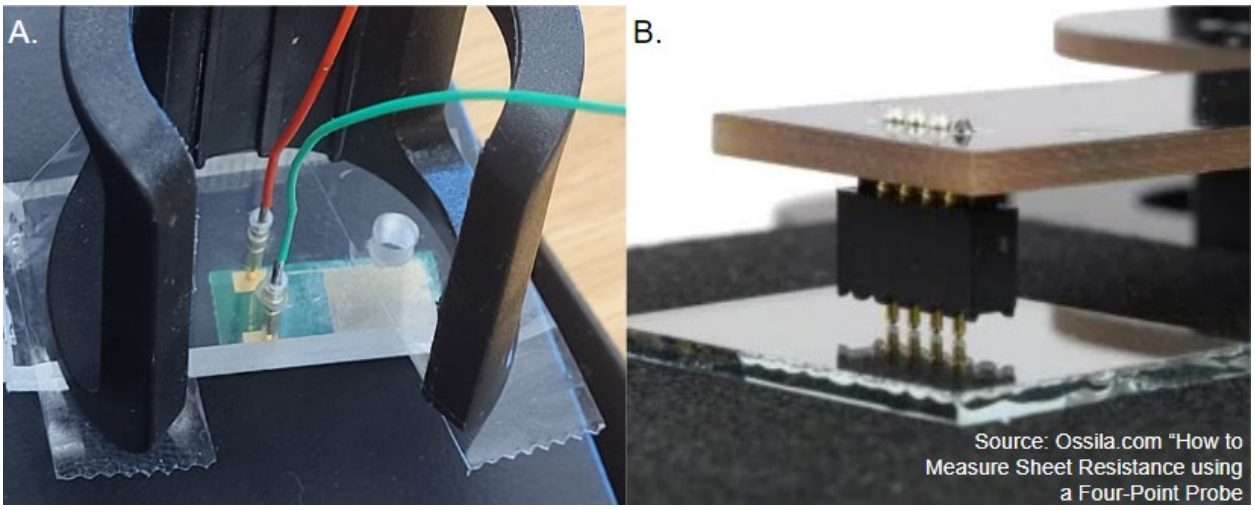

Figure 4. 2-probe (A.) and example of 4-probe (B.) gold pin measurements.

Key Results

ZnO Chemistry. The hydrothermal reactions successfully generate ZnO films onto glass substrates when zinc acetate and nitrate are used as precursors, Figure 5A, 5B. Conversely, when zinc sulfate is used, the product is zinc hydroxysulfate, 3 $Zn(OH)_2 \cdot ZnSO_4 \cdot H_2O$. Annealing these samples (see Methods) can transform the film into ZnO, Figure 5C.

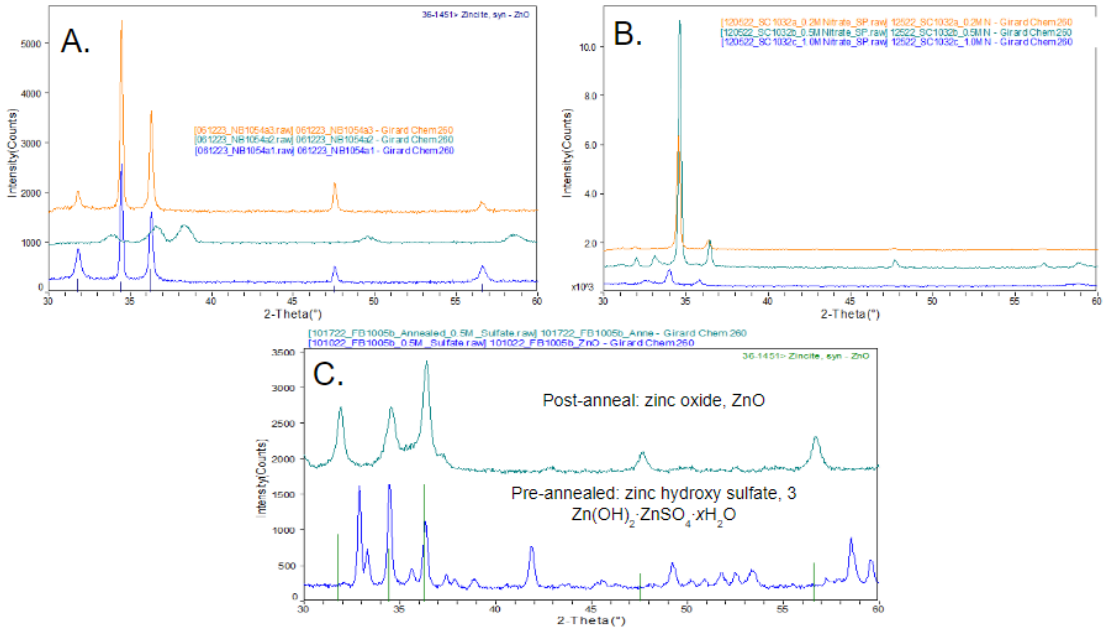

Figure 5. PXRD patterns of ZnO products generated from zinc acetate (A) and zinc nitrate (B). PXRD pattern of zinc hydroxysulfate product generated from zinc sulfate precursors. Upon annealing, the zinc hydroxysulfate transforms into ZnO (C).

The size and morphology of the ZnO nanostructures obtained vary considerably depending on the precursor used. ZnO samples synthesized with zinc acetate formed small hexagonal nanorods or even nanowires. ZnO samples with a zinc nitrate precursor tended to form hollow nanorods with appearances similar to honeycombs. Zinc sulfate precursor samples formed very thin wafer-like

hexagonal nanoplates. Combinations of zinc nitrate and zinc acetate also formed small nanorods. The difference in morphology when it comes to these samples is key to creating an effective gas sensor due to the change in surface area of each particle.

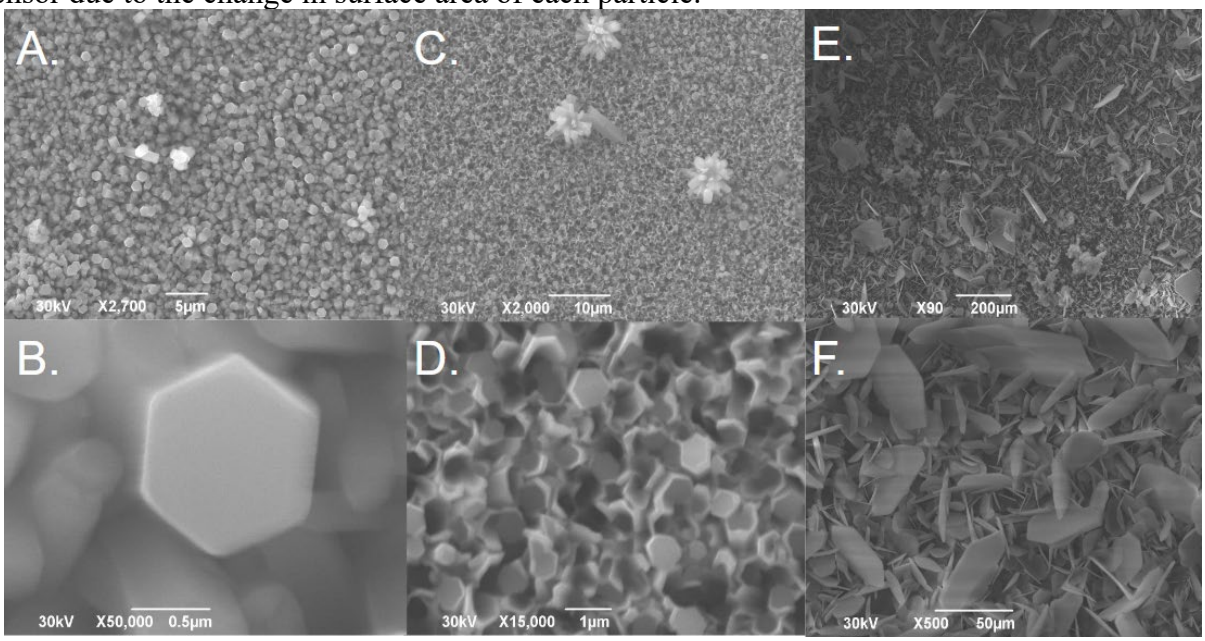

Figure 6. SEM analysis of ZnO samples generated using: A-B) zinc acetate, C-D) zinc nitrate, E-F) zinc sulfate precursors. Zinc acetate generates a dense coating of hexagonal nanorods, zinc nitrate generates hexagonal honeycombs, and zinc sulfate generates wide nanoplates.

Using the Debye-Scherrer equation $D = \lambda/\beta\cos\theta$ and incorporating the wavelength of the PXRD instrument as well as the 2-theta and β values of each peak, the average particle diameter can be determined (Table 1).

	Zinc acetate samples	Zinc nitrate samples
Number of samples analyzed	24	11
Avg. particle diameter (nm)	34.29	36.62
Standard Deviation (nm)	8.27	6.80
Range (nm)	30.60	22.41

Table 1. Statistics of particle diameters of various ZnO samples synthesized with either zinc acetate or zinc nitrate.

For some samples, sparse and incongruous coatings of ZnO can be observed on the glass substrate surface following the reaction. Variations of reagent concentrations show that the adherence of ZnO onto the substrate is a challenge, as displayed in Figure 7. For some samples, the films have poor adherence to the glass substrate, resulting in film cracking and delamination. In order for these samples to be used as gas sensors, the ZnO films obtained must demonstrate a homogeneous, unbroken coating and good adherence to the substrate.

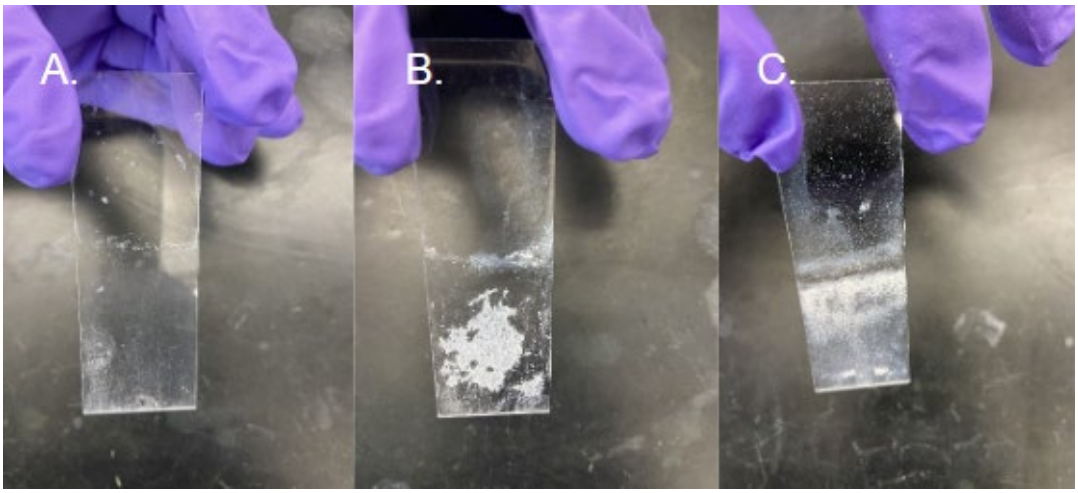

Figure 7. Substrates coated via only hydrothermal reaction (A). 0.2M zinc acetate (B). 0.5M zinc acetate (C). 1.0M zinc acetate.

Improving ZnO Film Quality.

To improve the adherence and homogeneity of the zinc oxide film, we utilized spray pyrolysis. This technique involves using aerosolized aqueous solutions of zinc salts that deposit a seed layer of ZnO on the glass substrate when heated to high temperatures. Subsequently, the seeded substrate then underwent the standard hydrothermal reaction. As shown in Figure 8, this significantly improved the density and uniformity of the zinc oxide on the substrate.

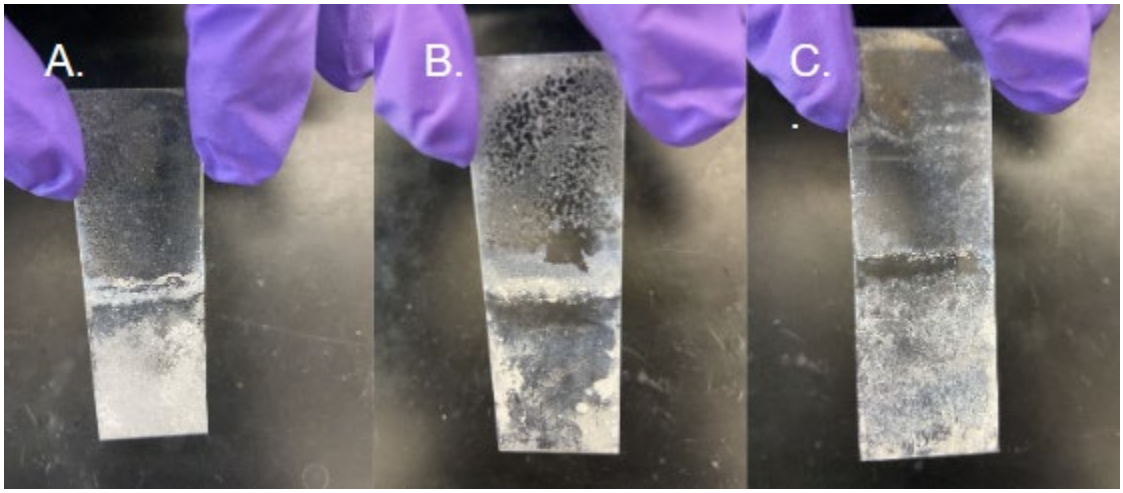

Figure 8. Substrates coated via spray pyrolysis prior to hydrothermal synthesis (A). 0.2M zinc acetate (B). 0.5M zinc acetate (C). 1.0M zinc acetate

Overall, the best concentrations for creating ZnO crystals on substrates ranged from 0.01M to 0.5M of both the zinc precursor salt and base. Concentrations that were too low formed very few crystals at all, but higher concentrations did not adhere well to the substrate and often flaked off of the glass entirely.

Through PXRD it can be observed that certain peaks are larger than others, specifically the second most peak, or the [002] position, located at ~34.5˚ 2θ, Figure 9A. This increased peak profile indicates preferential growth of crystals along the *c* axis of the ZnO crystals synthesized. The [002]

was heavily favored in many samples, pointing directly up and out of the substrate. The preferential growth is clearly shown via SEM, with the nanorods pointing directly at the screen, parallel to the *c* axis, Figure 9B.

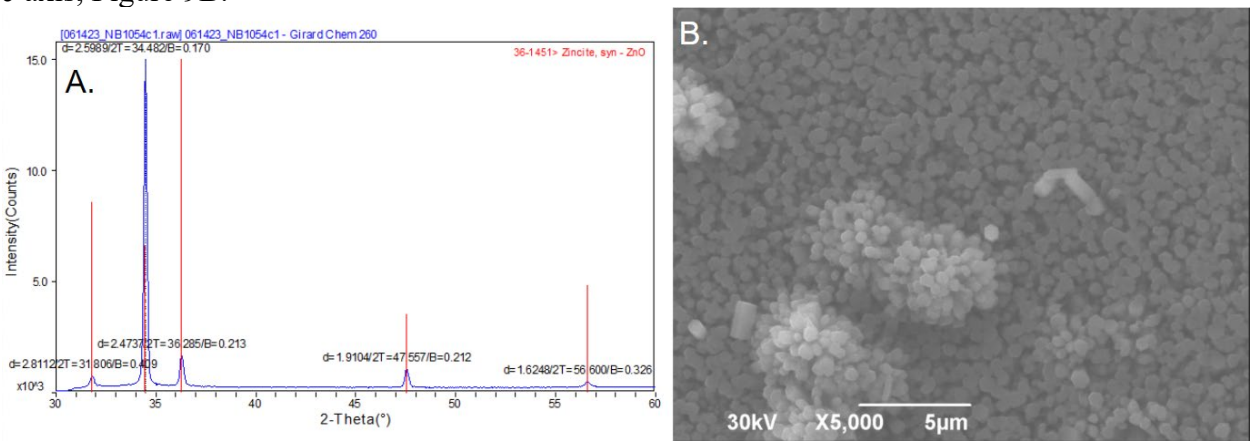

Figure 9. A ZnO sample synthesized with zinc acetate shows clear preferential growth in the second [002] peak (A). SEM images of this sample further confirm growth of crystals along the *c* axis (B).

Resistance Measurements and Development of ZnO Sensors. Initial resistance measurements of samples that underwent solely the hydrothermal process had a high resistance of over 1GΩ, indicating that large portions of the sample were essentially uncoated glass. After improving the film quality, the range of resistance data of zinc acetate samples reduced to 0.15-13 MΩ, and nitrate to 0.15-25 MΩ. Zinc sulfate samples produced significant variation in resistance, generally upwards of 200 MΩ. As a result, our sensor analysis has focused primarily on samples generated from zinc acetate and zinc nitrate.

When exposed to CO_2, many of the samples did not produce a notable response, regardless of the quality of the coating. Slight changes in current could be observed, but there was no clear trend, Figures 10A-C. It was also discovered during the preliminary measurements that the samples were displaying an increase in current when exposed to the fluorescent lights in the room. Even after darkening the surroundings of the instrument, many of the samples still held on to some of the energy from previous exposure.

In an attempt to improve sensing of these ZnO films, optimized ZnO was performed onto a gold interdigitated electrode (IDE) on printed circuit board material. It was theorized that the more conductive properties of the substrate would improve the sample sensitivity as opposed to the insulating effect of a glass substrate. The IDE solution concentration was 0.2 M for both the zinc nitrate precursor salt and the HMT base. Nitrate was chosen due to the high surface area in its crystalline morphology, correlating to a higher number of active sites for CO_2 to interact. The sample was synthesized without spray pyrolysis to avoid potentially damaging the delicate gold material. Upon initial viewing, the sample displayed an uneven coating, Figure 10E. However, once the sample was introduced to CO_2, there was a brief increase in current immediately followed by a steady downward sloping trend, marking an increase in resistance. The CO_2 was turned off to view the continuing effect, and the resistance continued to increase. When running a second trial, the same pattern could be seen. The results of this sample indicate an opposite response than what was previously predicted by Kanaparthi and Singh, Figure 10D. This analysis is ongoing to

determine the cause behind this effect or if it is repeatable. We also hope to investigate utilizing the IDE electrodes as substrates for zinc acetate sourced samples and spray pyrolysis deposition.

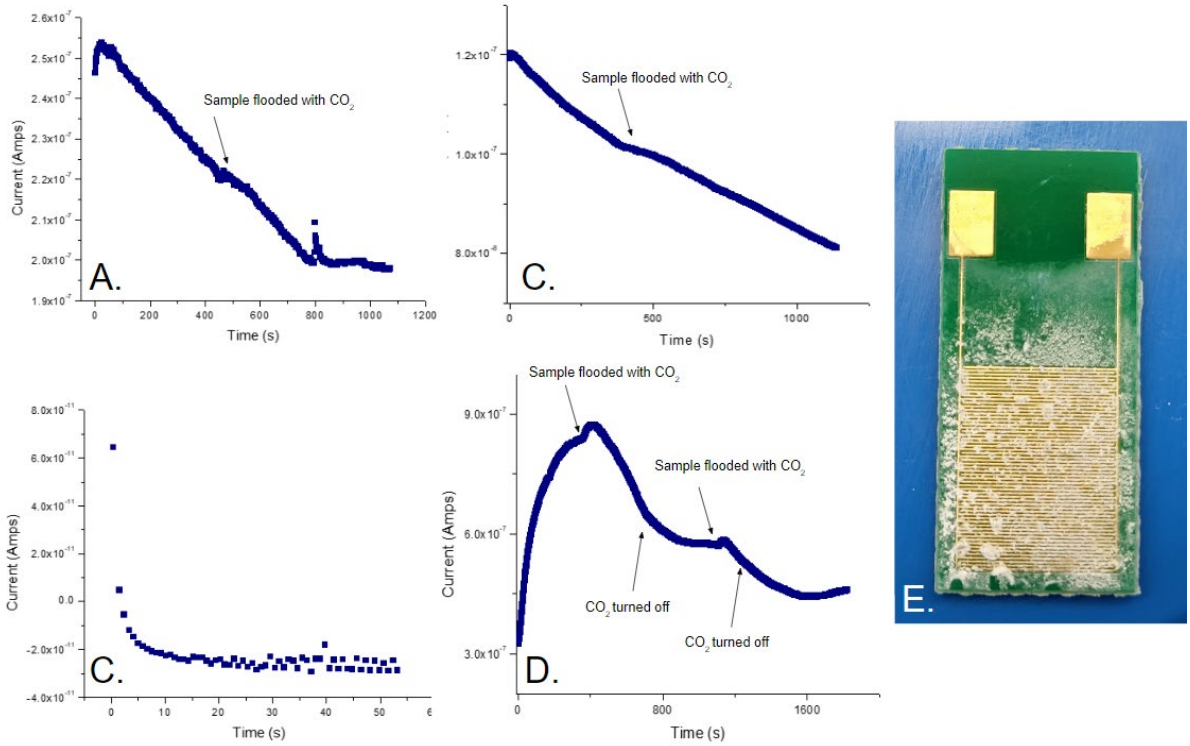

Figure 10. CO_2 testing Current vs. Time graphs of a zinc acetate (A), nitrate (B), and sulfate (C) sample. Testing results of the interdigitated electrode sample (D) and a photo of the coated IDE (E).

Discussion

We successfully demonstrated the controlled growth of ZnO crystals with a variety of different morphologies and sizes that were grown directly onto substrates. Additionally, we have demonstrated excellent film homogeneity and adhesion, improving their utility as sensors. With uniform and densely coated substrates the resistance tests were performed in order to determine the effectiveness of the sensors. Initial results show a difference in electrical resistance under CO_2 flow, indicating our nanostructured ZnO can serve as CO_2 sensors. However, the mechanism of this effect, and the sensitivity of the sensors, require further study.

Future endeavors to improve these sensors will include a more robust setup to block ambient UV light wherein samples are isolated from light for an extended period before measurement. Additionally, heating the sample as it is measured will be valuable, as this change would remove adsorbed oxygen from the surface wherein CO_2 could be flowed over the sensor and adsorb as the device cools.

Acknowledgments

We thank the WSGC for funding this work via a Higher Education Initiatives Grant, HEI21_3-0 made available through NASA Education Cooperative Agreement #80NSSC20M0123, and the UWW Undergraduate Research Program. We also thank Dr. Ozgur Yavuzcetin at UW-Whitewater for the use of his lab space and instruments for conducting both resistance and CO_2 measurements.

References

Kanaparthi, S. & Singh, S.G. (2019). Chemiresistive Sensor Based on Zinc Oxide Nanoflakes for CO_2 Detection. *ACS Applied Nano Materials, 2(2)*, 700-706. https://doi.org/10.1021/acsanm.8b01763

Korotcenkov, G. & Cho, B. K. (2017) Metal Oxide Composites in Conductometric Gas Sensors: Achievements and Challenges. *Sensors and Actuators B: Chemical, 244,* 182–210. https://doi.org/10.1016/j.snb.2016.12.117

NASA Glenn Research Center, (2023) Gas Sensors. *NASA Glenn Research Center Website,* https://www1.grc.nasa.gov/research-and-engineering/chemical-sensors/gas-sensors/

Ossila Ltd., How to Measure Sheet Resistance using a Four-Point Probe. *Ossila Website,* https://www.ossila.com/pages/four-point-probe-measurement-guide